Materials Science-Poland, *Vol. 26*, *No. 2*, *2008*

Nano-ceramic aspect of preparation and processing of zirconia nanopowders

W. PYDA*

AGH University of Science and Technology, Faculty of Materials Science and Ceramics,
al. Mickiewicza, 30-059 Cracow, Poland

The hydrothermal method of preparation of zirconia nanopowders was reviewed with respect to the influence of solution pH, mineralizer and TiO_2 concentration on the composition and morphology of zirconia crystallite phase. The pH dependence of both the ratio of the needle-shaped monoclinic to oval tetragonal zirconia nano-crystallites and CaO concentration in the zirconia solution has been described. Compressibility improvement and sinterability deterioration of zirconia nanopowders due to the presence of needle-shaped crystallites have been shown. Hydrothermal crystallisation of zirconia nanopowders with a mineralizer-dependent amount of the tetragonal and monoclinic zirconia polymorphs composed of oval and elongated crystallites with various ratios or plate-shaped crystallites has been discussed. The effect of TiO_2 on hindered hydrothermal crystallisation of zirconia solid solutions was shown. A potential of the *in-situ* method for shaping the nano-structure of the TiC/ZrO_2 composites has been presented. A slight effect of the carbon precursor and a significant one of the carbon incorporation way on the morphology of TiC in-situ inclusions have been documented.

Key words: *zirconia; nanopowder; nanocomposite; TiC; hydrothermal crystallisation*

1. Introduction

Zirconia ceramics, a truly remarkable group of materials, range from electrically insulating, mechanically weak pure monoclinic zirconia through the fast ion conducting stabilised cubic and tetragonal forms to the TZP and Mg-PSZ ceramics characterised by superb mechanical properties. The latter materials utilize benefits of the transformation toughening associated with the tetragonal (t) to monoclinic (m) phase transformation. Furthermore, zirconia brings a potential for nanotechnology development. The last 35 years of extensive studies of the zirconia systems have delivered a wealth of exciting results [1–3], also those usable in the nanotechnology. Developed methods of fabrication of zirconia micropowders with controlled chemical and phase compositions and morphology can be

*E-mail: pyda@uci.agh.edu.pl

easily adopted to produce zirconia nanopowders [4–6]. Reactivity of zirconia-based ceramics has been studied contributing to development of new methods of production of the zirconia matrix composites and nanocomposites [7–9].

This paper is devoted to a nano-technological aspect of the methods of fabrication of zirconia nanopowders. Selected factors influencing the chemical composition, morphology and structure of hydrothermally crystallised zirconia nanopowders have been described. The potential of the *in-situ* method for shaping the nano-structure of the TiC/ZrO_2 and $TiB_2/TiC/ZrO_2$ composites is shown.

2. Zirconia nanopowders crystallised under hydrothermal conditions

2.1. Effect of pH

The effect of pH of the mineralizer solution on chemical and phase compositions, morphology, compaction and sintering behaviour of zirconia nanopowders was studied using zirconia solid solutions doped with 6 mol % CaO. The nanopowders were fabricated by the co-precipitation method followed by hydrothermal crystallisation described in detail elsewhere [10]. Calcia-zirconia hydrogels were precipitated from aqueous solutions of zirconyl and calcium chlorides with a solution of NaOH free of Na_2CO_3, hydrothermally crystallised for 4 h under autogeneous water vapour pressure at 240±5 ^oC and at pH ranging from 8.2 to 12.4.

Two populations of zirconia nano-crystallites differing in shape are observed as revealed by TEM (Fig. 1). The population content depends on the solution pH. Oval and nearly isometric particles belong to the first population. The second one is composed of needle-shaped particles. It was arbitrarily assumed that an aspect ratio of the needle-shape crystallites exceeds a value of 1.6.

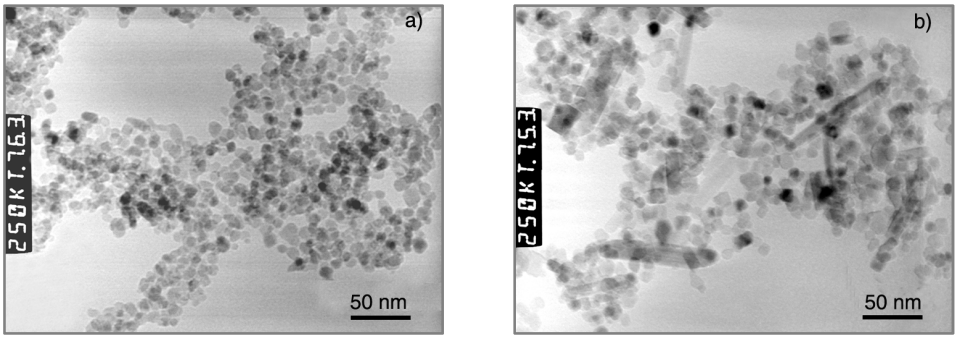

Fig. 1. SEM microphotographs of the 6 mol % $CaO–ZrO_2$ nanopowders crystallised at solution pH of: a) 8.2, b) 12.1

Oval crystallites prevail over the needle-shaped ones at any pH. Their sizes change slightly upon pH changes (Fig. 2). An increase of the average values from 9.3 nm to 14.0 nm has been found within the studied pH range. An aspect ratio of the

oval crystallites remains nearly constant in this pH range (Fig. 3) keeping an average value of 1.32±0.03. The needle-shaped crystallites triple their width from 7.3±0.8 nm to 20.5±7.8 nm (Fig. 2). Simultaneously, their length increases more than seven times reaching 102±39 nm. As a result, the aspect ratio increases to the value of 5.2±1.9.

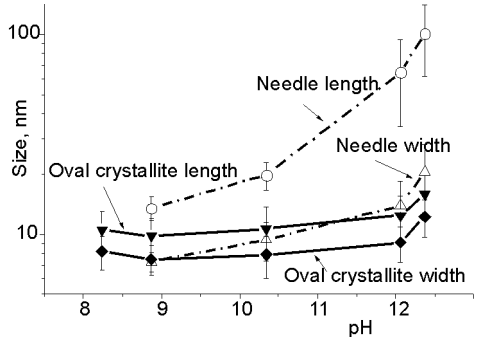

Fig. 2. Size of oval and needle-shaped crystallites in function of pH

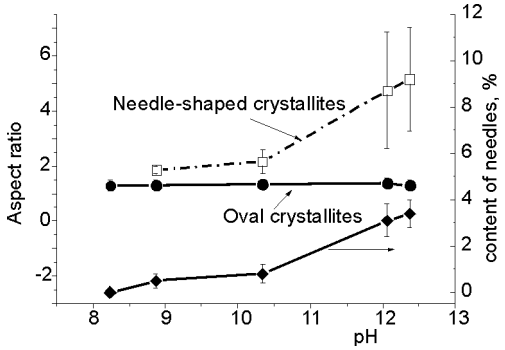

Fig. 3. Aspect ratio of oval and needle-shaped crystallites and number content of needle-shaped crystallites in function of pH

The crystallites which look like plates have been sporadically found in the zirconia nanopowders crystallised at pH 8.2 and 12.0. In this case, the average crystallite sizes are equal to 13.7±1.9 nm and 18.1±6.4 nm and aspect ratios to 1.37±0.12 and 1.30±0.22, respectively. The amount of CaO introduced into the zirconia solid solution during the hydrothermal treatment depends on the solution pH as is shown in Fig. 4. Only pH values higher than ~10.3 are suitable to retain CaO quantitatively in the zirconia nanopowder. The tetragonal and monoclinic zirconia polymorphs are present in the zirconia nanopowders (Fig. 4). The X-ray diffraction measurements reveal the tetragonal and monoclinic symmetries for the oval and needle-shaped crystallites, respectively. This is consistent with the finding that both the monoclinic phase content and number of the needle-shaped crystallites (Fig. 3) increase with pH.

The presented data indicate an in-situ transformation as the most probable crystallisation mechanism of tetragonal zirconia nanocrystallites suggested first by Adair et al. [11] for pure zirconia crystallising under hydrothermal conditions. This mechanism assumes a spontaneous transformation of amorphous zirconia hydrogel particles into a crystalline form with no dissolution-precipitation. A continuous and great increase of the needle-shaped particle aspect ratio with pH suggests a dissolution-precipitation mechanism for growth of monoclinic zirconia crystallites. Its contribution to development of the calcia –zirconia powder morphology increases with pH as a result of an increased zirconia solubility in the mineralizer solution. Tani et al. [12] and Bućko et al. [13] also reported this mechanism for hydrothermally grown pure zirconia crystallites.

The needle-shaped crystallites affect densification of zirconia nanopowders during compaction and sintering. The green density increases with pH reaching the value of

49.5 % of theoretical density for pH = 12.4 (Fig. 5). This is consistent with a general knowledge on densification of polymodal systems with controlled grain size distributions during compaction. An opposite dependence is observed for the density of a sintered body (Fig. 5). Therefore, the presence of needle-shaped nanocrystallites improves compressibility of the nanopowders but deteriorates their sinterability. The latter property is most probably related to the effects of both differential sintering and back stresses which can be generated by relatively large needles.

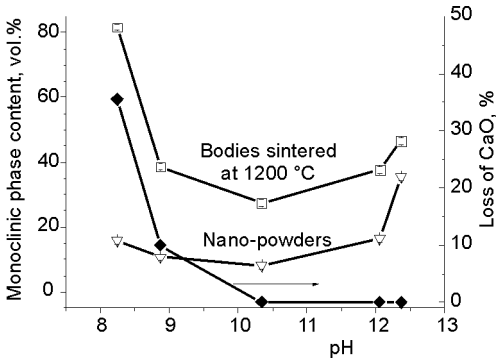

Fig. 4. Monoclinic phase content in 6 mol % CaO-ZrO_2 nanopowders and the bodies sintered at 1200 °C, and loss of CaO during zirconia hydrogel processing in function of pH

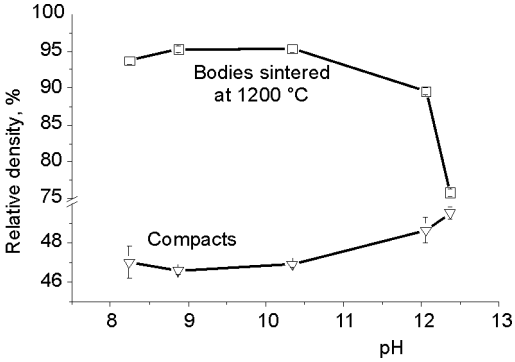

Fig. 5. Relative density of green compacts and bodies sintered at 1200 °C in function of pH

The phase composition of the sintered materials is shown in Fig. 4. Zirconia phases of the monoclinic and tetragonal symmetry are detected. A minimum exists in the dependence of monoclinic zirconia content on pH. An increase of the monoclinic zirconia content observed at pH lower than 10.3 is attributed to destabilisation of the zirconia solid solution due to the loss of CaO. An increase of the monoclinic zirconia content observed at pH above 10.3 is attributed to needle-shape crystallites which reduce sinterability of the zirconia nanopowder. This finding is crucial for fabrication of TZP materials stabilised with CaO indicating that zirconia nanopowders with the monoclinic phase content limited to minimum and containing nanocrystallites of slightly diverse shapes and sizes are only suitable for the production of tetragonal calcia–zirconia based materials and nanomaterials.

2.2 Effect of mineralizer on the zirconia nanopowder morphology

Zirconia nanopowders with no stabilizer were crystallised under hydrothermal conditions. Water, 1 M water solutions of NaCl, Na_2SO_4, $NaNO_3$ or Na_2CO_3 and saturated water solutions of $Na_2B_4O_7$ or NaF were used as mineralizers. Zirconia hydrogels were precipitated with ammonia, washed with water, mixed with the mineralizer and hydrothermally treated for 4 h at 250 °C under a saturated water vapour pressure at pH < 9.1.

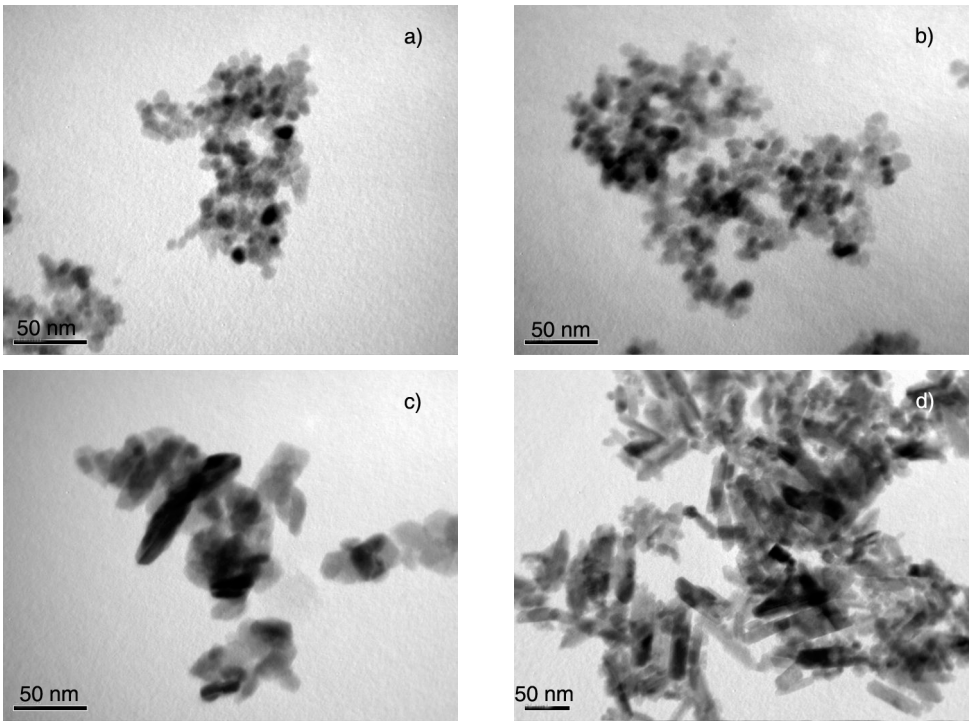

Fig. 6. Morphology of zirconia nanopowders depending on a mineralizer: a) H_2O, b) Na_2SO_4, c) NaF, d) Na_2CO_3

A strong dependence has been found of the morphology of zirconia nanopowder on the mineralizer applied. Nanopowders with a mineralizer dependent amount of the tetragonal and monoclinic zirconia polymorph composed of oval, elongated, a mixture of oval and elongated or plate-shaped crystallites were produced. The zirconia nanopowders derived from H_2O (Fig. 6a), NaCl (Fig. 6b), Na_2SO_4 and $NaNO_3$ crystallization environments are similar to one another having an oval crystallite shapes, a projection size of 10.3±0.4 nm, a specific surface area of 97±2 m^2/g, and tetragonal and monoclinic phase contents of 79±6% and 21±6%, respectively. NaF crystallisation environment leads to increased crystallites of the size ranging from 10 nm to 47 nm, nearly plate-shaped morphology (Fig. 6c) and solely monoclinic symmetry. The zirconia nanopowders crystallised in the $Na_2B_4O_7$ (Fig. 6d) and Na_2CO_3 environments were composed of both oval and needle-shaped crystallites. Monoclinic phase contents of 75.3 % and 80.9 %, oval crystallite projection sizes of 2.6–10.2 nm and 5.6–26.6 nm, needle-shaped crystallite projection sizes of 6.0–27.4 nm and 10.5–75.1 nm, the aspect ratios of the needle-shaped crystallites of 4.5 and 4.3 were measured for the nanopowders crystallised in the $Na_2B_4O_7$ and Na_2CO_3 environments, respectively. The presented results indicate that the $B_4O_7^{2-}$ ions inhibit growth of tetragonal crystallites and aid monoclinic but the CO_3^{2-} ions aid also some growth of the tetragonal crystallites.

The latter ions especially favour an increase of a monoclinic crystallite length. The value of 154 nm was measured being the largest for the studied nanopowders.

2.3 Effect of TiO_2 content on zirconia crystallisation

Hydrothermal crystallisation of zirconia solid solutions containing 3 mol % Y_2O_3 and 20–50 mol % TiO_2 with the step of 10 mol % was studied. Zirconia hydrogels were co-precipitated from aqueous solutions of appropriate chlorides with ammonia at pH = 9, washed with water and hydrothermally treated for 4 h at 250 °C under a saturated water vapour pressure at pH = 7.5.

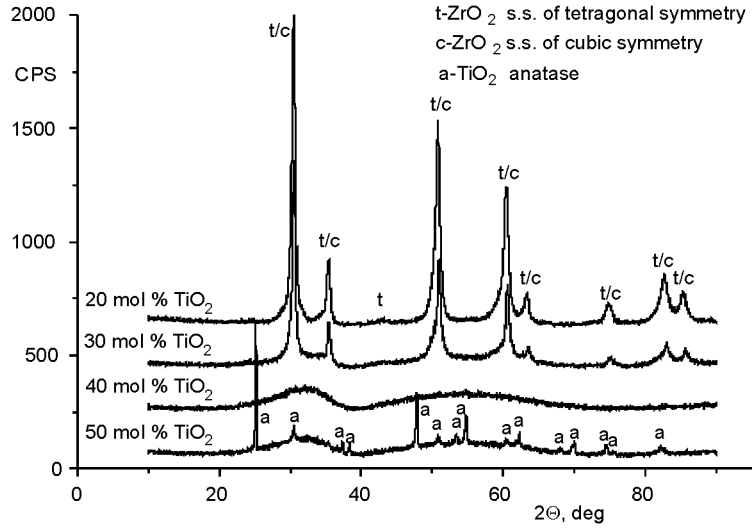

Fig. 7. X-ray diffraction patterns of the zirconia powders containing 3 mol % Y_2O_3 and the indicated TiO_2 concentration after hydrothermal crystallisation for 4 h at 250 °C

The X-ray diffraction measurements revealed TiO_2 playing a very important role in hydrothermal crystallisation of the zirconia solid solutions as shown in Fig. 7. TiO_2 contents exceeding 30 mol % hindered crystallisation of tetragonal and cubic polymorphs of the zirconia solid solution and left the zirconia hydrogel in an amorphous state accompanied additionally by anatase in the case of the 40 mol % TiO_2 sample. The results suggest that nuclei formation and growth of the TiO_2 rich phases, e.g., $ZrTiO_4$ requires temperatures and/or pressures higher than the applied ones.

2.4. An in-situ synthesis of the TiC and TiB_2 inclusions in the zirconia matrix

Carburisation of the zirconia structure and chemical reaction occur when carbon encounters with zirconia. Carbon easily diffuses throughout the zirconia lattice occupying the octahedral interstitial sites as a neutral atom [15]. Diffusion kinetics depends

on time and temperature. The process commences when the temperature exceeds 700 °C. The carburisation prevents degradation of tetragonal zirconia polycrystals doped with 3 mol % of yttria (3Y-TZP) in water or steam at 200 °C [15]. Heat treating of sintered 3Y-TZP in a carbon atmosphere resulted in a surface layer formation stabilised by carbon ions but the bulk strength was slightly decreased.

Carbothermal reduction of zirconia is another result of the interaction of carbon with zirconia solid solutions. The value of the standard Gibbs free energy of ZrC formation indicates that the carbothermal reduction of zirconia can occur at about 1627 ºC under CO partial pressure of 1 atm. Decreasing the CO partial pressure decreases the reaction temperature.

Titanium oxide forms a substitutive solid solution with zirconia which is well known and documented [16]. Titanium oxide segregation during the solution formation has been reported [17]. The segregation factor of 5 was determined within a layer extending up to 6 nm into the zirconia grain. The titanium segregation affects zirconia grain growth increasing the rate of growth. Finally, in some conditions titanium can reduce its valence and increase the oxygen vacancy concentration. This affects the phase composition of zirconia polycrystals increasing the amount of the cubic zirconia polymorphs which do not participate in transformation toughening. Titanium oxide dissolved in the zirconia structure is subject to carbothermal reduction at 1280 °C under CO partial pressure of 1 atm as indicated by the thermodynamic calculations [7, 8]. This temperature, being lower than that of zirconium carbide formation, provides opportunity to carbonise TiO_2 selectively while leaving ZrO_2 unchanged. Therefore, a new process aiming at preparing tetragonal zirconia powders containing titanium carbide was developed at the AGH University of Science and Technology in 1998 [7]. A year later, Liu et al. reported similar studies [18]. The process was further developed to produce titanium diboride inclusions in the zirconia matrix [19]. This new approach provides methods to control the morphology and size of the inclusions via a control of nucleation and nuclei growth opposite to the physical mixing method in which reduction of the reinforcement particle size proceeds. Therefore, it is attractive for production of the zirconia based transformation toughened composites and nano-composites reinforced with hard and stiff inclusions.

The preparation route of the zirconia matrix composites with in-situ TiC and/or TiB_2 inclusions utilises benefits of the TiO_2 doped zirconia nanopowders produced by the co-precipitation method followed by calcination or hydrothermal treatment. The original zirconia nanopowder is homogenised with a carbon precursor, e.g., phenol-formaldehyde resin [7, 9], sucrose [18] or carbon nanotubes and a boron precursor in the case of the $TiB_2/TiC/ZrO_2$ composites [19]. The *in-situ* synthesis is performed at temperatures ranging from 1000 °C to 1650 °C in argon or under vacuum. The composite powder is always ground to receive an appropriate sinterability.

A method of surface carburisation of dense tetragonal zirconia polycrystals combined with carbothermal TiO_2 reduction has also been reported [8]. The presence of both TiC and TiB_2 *in-situ* inclusions affects sintering of titania–zirconia nanopowders.

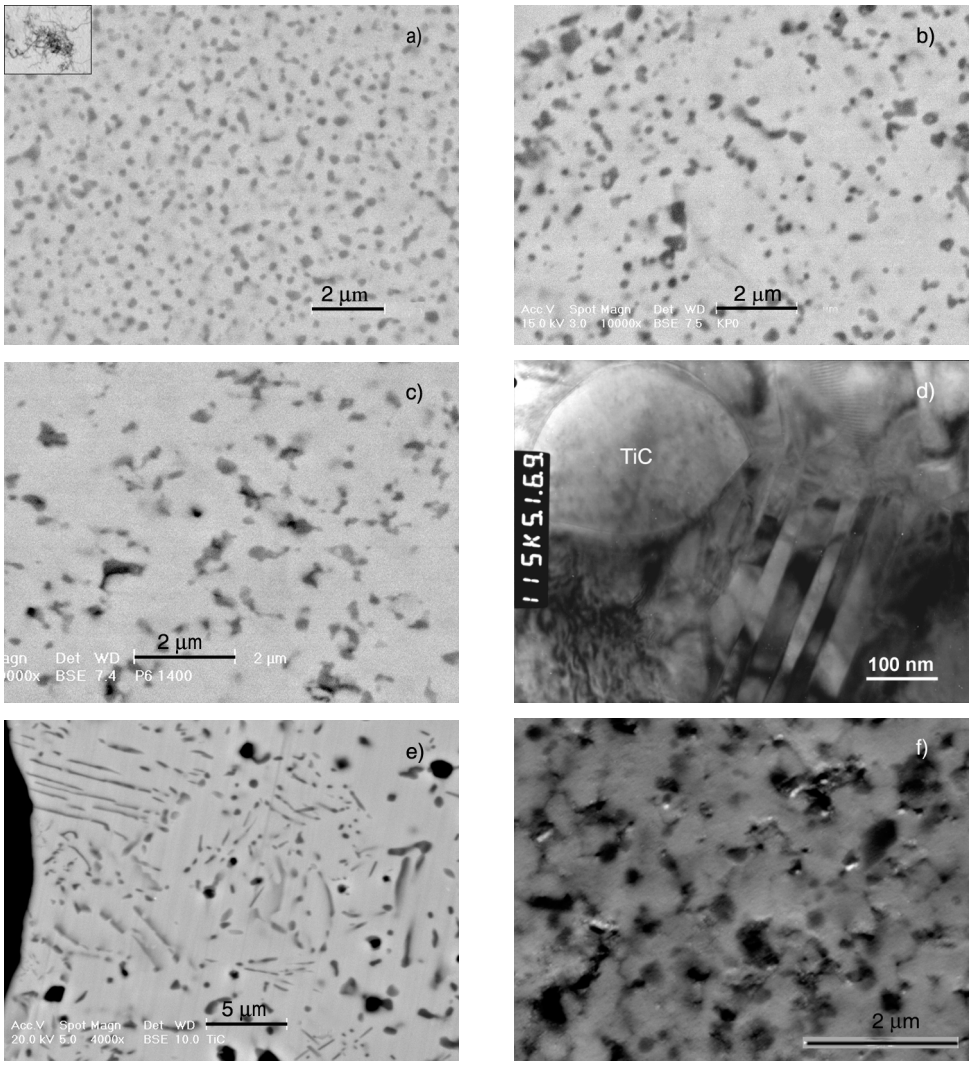

Fig. 8. Morphology of the in-situ inclusions depending on the carbon precursor (PF – phenol–formaldehyde resin, CNT – carbon nanotubes), processing (B – bulk synthesis, S – surface carburisation) and sintering temperature: a) 10.2 wt. % TiC–ZrO_2, B, 1500 °C, b) 10.7 wt. % TiC–ZrO_2 – PF, B, 1500 °C; c) and d) TiC–ZrO_2–PF, B, 1400 °C, e) ~10 wt. % TiC–ZrO_2%–PF, S, 1650 °C, f) 12.9 vol. % TiB_2, 8.9 vol.% TiC–ZrO_2–PF, H_3BO_3, B, 1500 °C

The inclusions inhibit grain growth by a pinning effect leading to a decreased densification. The composites derived from the nanopowders with unreacted carbon exhibit increased porosity due to CO which evolves when the additional amount occurs of the carbothermal TiO_2 reduction.

Hardness improvement (18.3±1.0GPa) of the surface carburised TZP has been reported [8]. Promising fracture toughness (K_{Ic}=8.8 ±0.5 MPa·$m^{0.5}$) and bending strength

(σ = 912±72 MPa) were obtained for not optimised composites with *in-situ* TiC and TiB_2 inclusions [19].

Morphological diversities of the *in-situ* inclusions depending on the carbon precursor and processing conditions are shown in Fig. 8. A comparison of Figs. 8a and 8b indicates a slight effect of the carbon precursor morphology on the morphology of the TiC *in-situ* inclusions. However, the way of introducing carbon, i.e., surface or bulk carburisation, was found to be a significant factor influencing the TiC inclusion shape (Fig. 8e).

3. Concluding remarks

The results presented show that the hydrothermal method of fabrication of zirconia nanopowders is a real example of the ceramic nanotechnology. pH of the solution, type of mineralizer and TiO_2 concentration belong to factors influencing composition and morphology of the zirconia crystallite phase. However, processing the zirconia nanopowders to nanoceramics is not an easy task. Even very sophisticated methods of nanocomponent homogenisation do not lead to fully nanostructural materials if high temperature treatment is applied. This is proved by the results of the *in-situ* synthesis of TiC inclusions by using carbon nanotubes or carbon delivered by phenol -formaldehyde resin. A TiC inclusion size touching the nanometric limit was only obtained. However, when benefits of the carbon diffusion through the zirconia lattice are fully utilized, the real nanometric in-situ TiC is produced as a surface carburisation method shows.

Acknowledgements

Financial support from the resources allocated for science in 2006–2008 under the grant No. N507 017 31/0527 has been provided for this research work.

References

[1] *Science and Technology of Zirconia I*, Vol. 3, A.H. Heuer, L.W. Hobbs (Eds.), The American Ceramic Society, Columbus, OH, 1981.
[2] *Science and Technology of Zirconia II*, Vol. 12, N. Claussen, M. Rühle, A.H. Heuer (Eds.), The American Ceramic Society, Columbus, OH, 1984.
[3] *Science and Technology of Zirconia V*, S.P.S. Badwal, M.J. Bannister, R.H.J. Hannink (Eds.), Technomic Publ. Co., Lancaster, Basel, 1993.
[4] BYRAPPA K., YOSHIMURA M., *Handbook of Hydrothermal Technology*, Noyes Publications, William Andrew Publ. LLC, USA, 2001, Chapter 1.2.
[5] SOMIYA S., ROY R., Bull. Mater. Sci., 23 (2000), 453.
[6] PYDA W., HABERKO K., BUĆKO M. M., J. Am. Ceram. Soc., 74 (1991), 2622.
[7] PYDA W., [in:] Proc. II ICCST, S. Adali, E.V. Morozov, V.E. Verijenko (Eds.), 3–11 June 1998, Department of Mechanical Engineering, University of Natal, Durban, 1998, 195.
[8] HABERKO K., PYDA W., PĘDZICH Z., BUĆKO M.M., J. Eur. Ceram. Soc., 20 (2000), 2649.

[9] PYDA W., Ceramics Int., 30 (2004), 333.
[10] PYDA W., *Advances in Science and Technology*, Vol. 45, Trans Tech Publications, Switzerland, 2006, pp.194–199.
[11] ADAIR J. H., DENKEWICZ R.P., ARRIAGADA F. J., OSSEO-ASARE K., [in:] *Ceramic Powder Science II*, G. L. Messing, E. R. Fuller, H. Hausner (Eds.), The American Ceramic Society, Inc. Westerville, OH, 1988, p. 135.
[12] TANI E., YOSHIMURA M., SOMIYA S., J. Am. Ceram. Soc., 66 (1983), 11.
[13] BUĆKO M. M., HABERKO K., FARYNA M., J. Am. Ceram. Soc., 78 (1995), 3397.
[14] NISHIZAWA H., YAMASAKI N., MATSUOKA K., MITSUSHIO H., J. Am. Ceram. Soc., 65 (1982), 343.
[15] ZHAO Z., LIU C., NORTHWOOD D.O., J. Aust. Ceram. Soc., 36 (2000), 135.
[16] BANNISTER M.J., BARNES M.J., J. Am. Cram. Soc., 69 (1986), C269.
[17] ALLEMANN J.A., MICHEL B., MÄRKI H.-B., GAUCKLER L.J., MOSER E.M., J. Eur. Ceram. Soc., 15 (1995), 951.
[18] LIU J., LI J., WANG H., HUANG Y., J. Am. Ceram. Soc., 82 (1999), 1611.
[19] MOSKAŁA N., PYDA W., Kompozyty (Composites), 5 (2005), 56.

Received 28 April 2007
Revised 16 February 2008